nature geoscience

LETTERS

PUBLISHED ONLINE: 27 FEBRUARY 2014 | DOI: 10.1038/NGEO2082

Modern and glacial tropical snowlines controlled by sea surface temperature and atmospheric mixing

Aradhna K. Tripati[1]*, Sandeep Sahany[1], Dustin Pittman[1], Robert A. Eagle[1], J. David Neelin[1], Jonathan L. Mitchell[1] and Luc Beaufort[2]

During the Last Glacial Maximum, tropical sea surface temperatures were 1 to 3 °C cooler than present[1–4], but the altitude of the snowlines of tropical glaciers[5,6] was lower than would be expected in light of these sea surface temperatures. Indeed, both glacial and twentieth-century snowlines seem to require lapse rates that are steeper than a moist adiabat[7,8]. Here we use estimates of Last Glacial Maximum sea surface temperature in the Indo-Pacific warm pool based on the clumped isotope palaeotemperature proxy in planktonic foraminifera and coccoliths, along with radiative–convective calculations of vertical atmospheric thermal structure, to assess the controls on tropical glacier snowlines. Using extensive new data sets for the region, we demonstrate that mean environmental lapse rates are steeper than moist adiabatic during the recent and glacial. We reconstruct glacial sea surface temperatures 4 to 5 °C cooler than modern. We include modern and glacial sea surface temperatures in calculations of atmospheric convection that account for mixing between rising air and ambient air, and derive tropical glacier snowlines with altitudes consistent with twentieth-century and Last Glacial Maximum reconstructions. Sea surface temperature changes ≤3 °C are excluded unless glacial relative humidity values were outside the range associated with deep convection in the modern. We conclude that the entrainment of ambient air into rising air masses significantly alters the vertical temperature structure of the troposphere in modern and ancient regions of deep convection. Furthermore, if all glacial tropical temperatures were cooler than previously estimated, it would imply a higher equilibrium climate sensitivity than included in present models[9,10].

The West Pacific warm pool is the warmest open ocean region with mean sea surface temperatures (SSTs) >29 °C (Fig. 1). It is an important source of water vapour and heat to the atmosphere, and a principal site of deep convection. The temperature structure of this region influences and is affected by the Walker circulation, which connects it with the El Niño–Southern Oscillation and the East Asian and Australian monsoons. The response of warm pool temperatures to changing forcing is a target for simulations, with Last Glacial Maximum (LGM) data used to test the accuracy of representations of oceanic and atmospheric processes in models[2,11,12]. Although many proxies have been used to estimate LGM SSTs, the magnitude of warming in the region is still unclear[1–4]. Several studies, including a recent synthesis, have inferred average regional ΔSSTs of ~1 °C (refs 1,2; Fig. 2a). Foraminiferal Mg/Ca ratios are interpreted to record a mean regional warming of

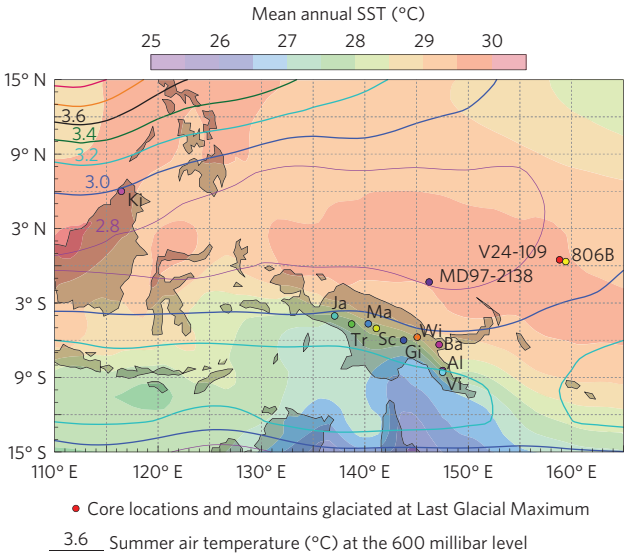

Figure 1 | Sites studied. Shown are core locations (806B, MD97-2138, V24-109) and mountains that were glaciated at the LGM (Tr, Trikora; Ki, Kinabalu; Gi, Giluwe; Wi, Wilhelm; Vi, Victoria; Ba, Bangeta; Ma, Mandala; Ja, Jaya; Sc, Scorpio; Al, Albert Edward). Annual average SSTs (ref. 22) are shown, with seasonal variability typically <0.4 °C. Average summer air temperature data (lines) indicate that temperatures at the 600 millibar level[22] over islands in the region are typically not more than a couple of tenths of a degree different from the same pressure level over the ocean.

~3 °C (refs 2–4). Salinity-corrected Mg/Ca temperatures indicate ~4 °C changes[13]; South Pacific coral Sr/Ca estimates are ~5 °C (ref. 14). Over land, warming of ~4–5 °C was reconstructed from thermodynamically based proxies (noble gases in groundwater) and purely empirically calibrated methods (pollen)[7,15].

Tropical glacial snowlines provide additional information on temperatures[5,6]. In the warm pool, snowlines approximate the freezing level heights, linked to SSTs and air temperatures at sea level (T_S) by tropospheric lapse rates. Over the tropical oceans, it is typically assumed the temperature structure of the atmosphere follows an adiabat to the freezing level[8,16]. We re-evaluated published data and found an adiabat cannot reconcile twentieth-century warm pool temperatures and snowline data (Fig. 3a). A moist adiabat initiated with modern T_S and surface relative humidity values

[1]Department of Earth, Planetary, and Space Sciences and Department of Atmospheric and Oceanic Sciences, Institute of the Environment and Sustainability, Institute of Geophysics and Planetary Physics, California Nanosystems Institute, UCLA, Los Angeles, California 90095, USA, [2]CEREGE, CNRS/Aix-Marseille University, Aix-en-Provence Cedex 4, France. *e-mail: aradhna.tripati@gmail.com

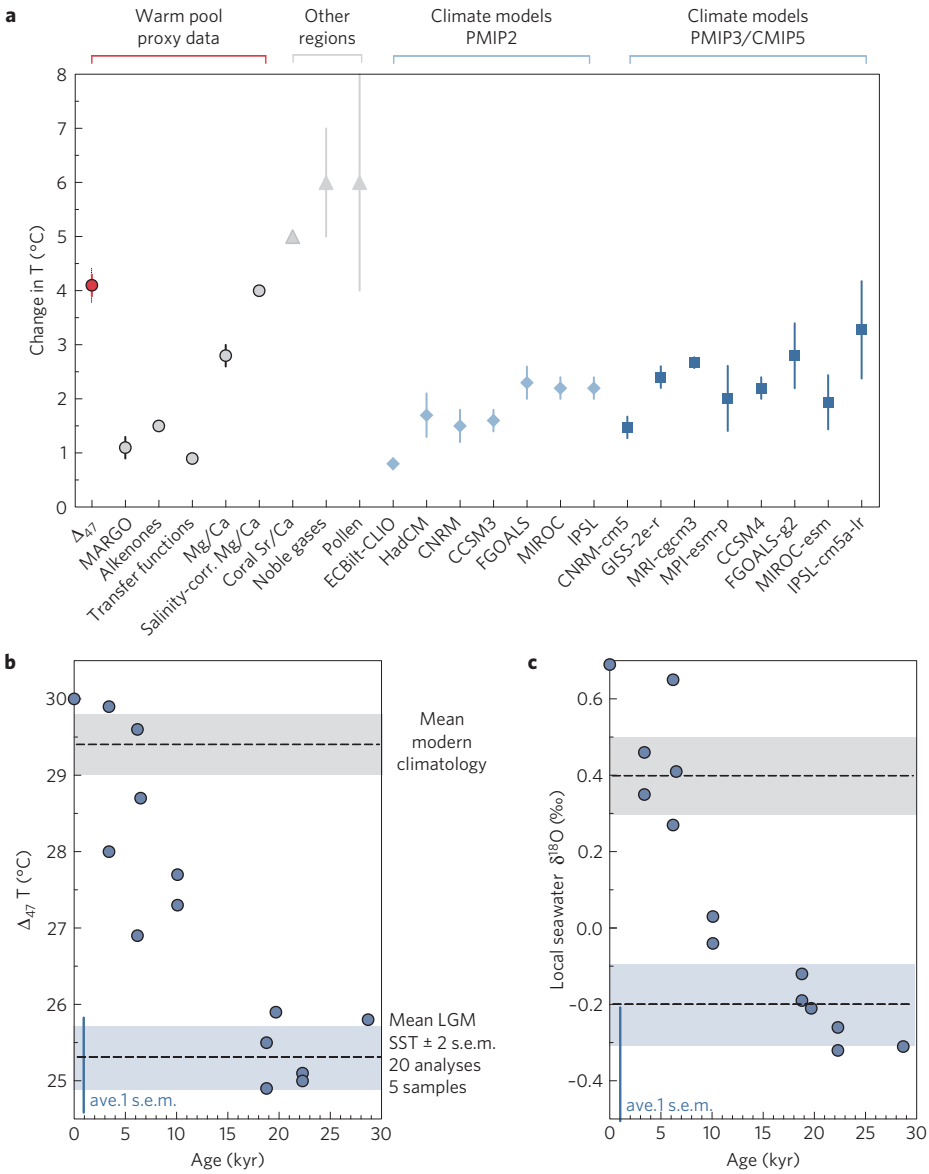

Figure 2 | LGM–recent changes in warm pool. a, Many sites and samples were used to develop statistically robust regional estimates. Values shown are calculated to be consistent with MARGO (ref. 2), which reported Δ SSTs = mean annual $SST_{climatological}$ − LGM proxy SST_{LGM} (Δ_{47} difference is 4.1 ± 0.4 °C (2 s.e.m.), $SST_{coretop} - SST_{LGM}$ is 4.7 ± 0.8 °C (2 s.e.m.)). 1 s.e.m. Δ_{47}, Mg/Ca, alkenone, transfer function error bars shown (Δ_{47} black line = 2 s.e.m.); Sr/Ca: range. Model ΔSSTs (refs 9,10) show LGM − pre-industrial annual mean (15° N–15° S, 140–165° E); vertical bars indicate spatial variability at core locations. **b**, LGM temperatures are 25.3 ± 0.4 °C (2 s.e.m.). Temporal variation is similar to Mg/Ca records[4]. **c**, Ice volume-corrected $\delta^{18}O_{seawater}$.

predicts a freezing level substantially higher than observations from four different sources (Methods). Differences between freezing levels predicted using a moist adiabat and observations are almost ten times greater than temperature sounding uncertainties (Fig. 3a and Supplementary Table 4). As with the modern, we find that a range of published values for LGM SSTs and snowline elevations (~3,600–3,700 m; refs 5,6,17,18) are inconsistent with a moist adiabat (Fig. 3b and Supplementary Table 5), consistent with previous studies[7,8]. Furthermore, reconciling small ΔSSTs with snowline changes (0.9–1.0 km after correcting for sea level) using a moist adiabat requires large changes in surface relative humidity and precipitation[19], lifting condensation level heights and the atmospheric boundary layer for this region that are unreasonable[20].

To understand changes in both the elevation of snowlines since the LGM and the absolute height of glacial and recent snowlines, we developed warm pool temperature estimates using clumped isotope (Δ_{47}) thermometry[21] (an innovation in stable isotope geochemistry) and combined estimates of SSTs with vertical structure calculations incorporating effects of entrainment (the process describing rising air within clouds drawing in and mixing with environmental air) on moist convection. Coretop data reproduce modern SSTs; LGM values indicate SSTs were 25.3 ± 0.4 °C (2 s.e.m.), 4.1 ± 0.4 °C (2 s.e.m.) cooler than modern climatological SSTs (ref. 22; Fig. 2). Results are most consistent with salinity-corrected Mg/Ca estimates for ΔSSTs in the warm pool[13] and are slightly greater than conventional Mg/Ca interpretations[2–4,23]. The magnitude of warm pool warming from Δ_{47} is similar to deep-water reconstructions[24]. If we take a reconstruction for the eastern equatorial Pacific from a recent synthesis[2] at face value, then similar SST changes may have occurred on both sides of the Pacific since the LGM.

We use Δ_{47}-derived $\delta^{18}O_w$ estimates to examine whether there is evidence of convective changes since the LGM. Locally, LGM

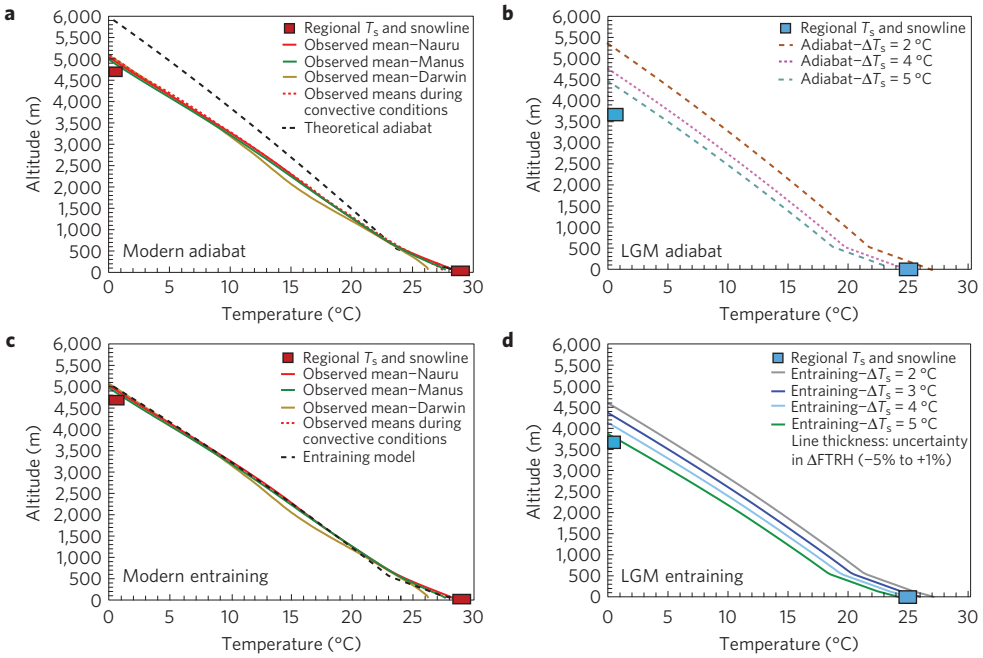

Figure 3 | Temperature profiles. Squares indicate regional averages from data. **a**, Mean vertical temperature profiles and late-twentieth-century snowlines. Soundings have uncertainties of <0.5 °C; snowline uncertainty smaller than symbol. An adiabat (T_s = 28.8 °C, surface relative humidity = 81%) departs substantially from freezing level. **b**, LGM estimates of snowlines and T_s (assuming <0.6 °C offset from Δ_{47} SSTs) compared with predicted profiles. Adiabats using ΔT_s = 2–5 °C depart substantially from snowlines (Supplementary Table 5). **c**, Entraining radiative–convective equilibrium model. **d**, Predicted LGM profiles factoring in entrainment, ΔT_s of 2–5 °C, and FTRH uncertainties. LGM snowlines are consistent with 4–5 °C of ΔSSTs (similar to Δ_{47} data).

surface waters were 0.7 ± 0.2‰ (2 s.e.m.) more depleted (than Late Holocene averages), which could reflect changes in moisture transport by the Walker cell. If evaporation was reduced locally and/or there was greater precipitation during the LGM, then more vapour must have been transported in from elsewhere (presumably from farther out in the Pacific or Indian Ocean). If increased rainout occurred, resulting in enhanced distillation, then ^{18}O-depleted vapour would be delivered to the warm pool at the LGM. Although vapour from the Pacific would have been more depleted if there was a stronger Walker cell, vapour originating from the Indian Ocean may have experienced increased rainout at the LGM due to exposure of the Sunda Shelf. Irrespective of the cause of the $\delta^{18}O_w$ signal, the relatively small magnitude shift implies there was not a dramatic change in convective regime since the LGM, consistent with the warm pool being one of the warmest open ocean regions throughout the Pleistocene.

Our SST reconstruction implies that T_S have warmed by ~4–5 °C since the LGM (range based on 95% confidence bounds; Supplementary Table 3). Although Δ_{47}-derived SST changes are sufficiently large to explain the 950 ± 50 m retreat of snowlines since the LGM (Fig. 3a,b), an adiabat still cannot reconcile the absolute height of LGM snowlines with our new constraints on T_S. Thus by combining Δ_{47} SSTs with snowline-based estimates for LGM freezing level height, we are able to confidently conclude that mean lapse rates in the free troposphere over the warm pool must have been steeper (more unstable) than the moist adiabat, as we concluded for the modern.

To explore what sets absolute regional snowline elevations, we assessed the influence of entrainment on modifying the equilibrium temperature structure of the lower troposphere and driving deviations from a moist adiabat in the LGM and the recent. This mechanism has not been proposed to resolve observations of modern SSTs with snowlines, or in palaeoclimate studies. Convection plays the dominant role in governing the vertical temperature structure over the warm pool. Recent observations and modelling studies of modern data sets show the process has a strong dependence on free tropospheric humidity that occurs through entrainment of air into convecting air parcels, with the onset of precipitating deep convection and cloud-top height matched only if substantial entrainment is considered[25–27].

Modern data can be matched using a modified radiative–convective equilibrium model with observed relative humidity and entrainment values typical of recent estimates (Fig. 3c). Entrainment of subsaturated air in the lower troposphere effectively changes parcel temperatures as they rise, driving deviations from a moist adiabat that accumulate with increasing altitude and resulting in substantial differences (~1 km) relative to freezing levels calculated from adiabats initiated with similar T_S values.

For the LGM, we are able to straightforwardly reconcile absolute values of Δ_{47} SSTs (25.3 ± 0.4 °C) with snowlines (3.6–3.7 km) using entrainment rates calibrated against modern data (Fig. 3d). For comparison, substantially erroneous LGM snowlines of ~4.4–4.5 km are predicted using an adiabat (Fig. 3c and Supplementary Table 5). Absolute snowline elevations for the LGM can be explained by SSTs similar to the proxy data (of 24.5–25.5 °C, implying ΔT_S = 4–5 °C) and free tropospheric relative humidity (FTRH), surface relative humidity and entrainment coefficient values that were similar to modern. Even after taking into account entrainment, snowline elevations are inconsistent with LGM SSTs of 26.5 °C or warmer; large FTRH changes (>10%) would be required, outside of the range associated with severe changes in convective regime in the modern. These relative humidity changes would also have to apply over a substantial portion of the warm pool. With ΔSSTs = 2 °C and a constant relative humidity, the predicted snowline retreat (~475 m) is half of what is observed.

The impact of uncertainties in entrainment, surface relative humidity and FTRH are relatively small compared with those stemming from SSTs. Model uncertainties in determining the modern entrainment coefficient, when propagated through for the LGM, are smaller than error bars on LGM snowlines. To reconcile

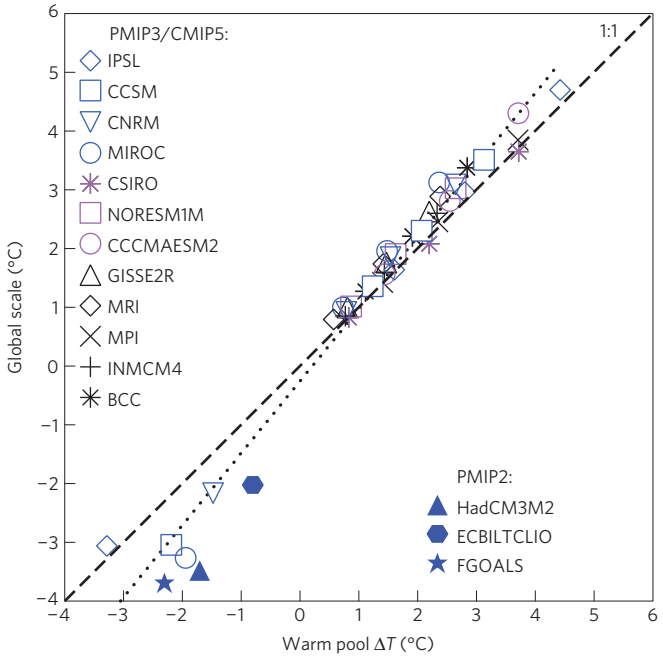

Figure 4 | Comparison of simulated changes in regional SSTs with global-scale changes for past and future. The significant correlation ($r^2 = 0.97$, $p < 0.0001$) suggests the warm pool temperature response may serve as a robust proxy for estimating global-surface temperature changes. Warm pool values for 15° N–15° S, 140 °–165° E; global scale changes for 50° N–50° S (excluding polar regions). Temperature differences calculated relative to the 1901–1960 base period. PMIP2 values are for the last 30 years of LGM simulations; PMIP3 and CMIP5 values are computed for 30-year intervals (2010–2039, 2040–2069 and 2070–2099) from RCP8.5 (high emission scenario). Regression (dotted line; slope 1.226 ± 0.035, intercept -0.257 ± 0.076) and 1:1 lines shown.

LGM observations of snowlines with Δ_{47} SSTs requires little to no change in entrainment, consistent with $\delta^{18}O_w$ data described above and the physical hypothesis that convective turbulence properties do not change. Nonetheless, we test sensitivity of freezing height calculations to entrainment coefficient. Predicted snowlines decrease ~60 m for every 10% increase in entrainment coefficient, if relative humidity profiles are kept invariant. LGM entrainment coefficient values similar to modern are consistent with 24.5 °C SSTs; values 120% of modern would be consistent with 25.5 °C SSTs. Small changes in surface relative humidity will affect snowlines, with a 2% decrease resulting in ~80 m of lowering. ~2–4% surface relative humidity changes are implied by models that show a scaling of 1–2% per °C (ref. 20); values are strongly constrained by boundary layer balances and oceanic moisture supply. Figure 3d shows the range of lapse rates and snowline changes associated with FTRH changes of −5% to +1%, representing conservative error bars that are > 2× the regional LGM changes occurring in model simulations; error bars in snowlines arising from uncertainties in FTRH are small (equivalent to changing T_S by 0.1–0.2 °C).

Here we provide new insights into the response of tropical SSTs and tropospheric structure to a changing climate, with the first application of clumped isotopes to Pleistocene palaeoceanography. It has two components that allow us to reconcile observations of LGM SSTs with snowlines. The large change in snowline elevations is explained by ΔSSTs and $\Delta T_S = 3–5$ °C. The absolute LGM snowline heights and absolute lapse rates require cool SSTs similar to the Δ_{47} data (~24.5–25.5 °C; $\Delta T_S = 4–5$ °C) and entrainment to be explained. Therefore we conclude LGM snowline data are consistent with the new Δ_{47} constraints on SSTs, 2–4% reduced surface relative humidity and entrainment rates similar to or slightly greater than modern.

Thus by combining thermodynamically based SSTs with tropical snowline data and a process that has not been discussed in any study of palaeoclimate, convective entrainment of environmental air, we have confirmed the mean LGM temperature structure over the warm pool is steeper than moist adiabatic, as in the modern. The wide array of constraints on temperature profiles over oceanic and terrestrial sites, including the analysis of extensive modern data sets, clearly demonstrates that in reality, the vertical structure of the lower troposphere does not follow a theoretical adiabat. This work supports studies that have incrementally moved away from an undiluted moist adiabat[25–27]. These findings are unlikely to be local as wave processes in the equatorial regions quickly minimize temperature differences in the horizontal, one of the primary reasons for similarity of modern profiles for sites ranging in continental proximity. Our treatment of modern and glacial atmospheric processes provides a significant mechanistic insight into climate relevant to the study of convective regions at all latitudes.

The interdisciplinary approach here, using a new combination of modern and geologic data in combination with modelling, resolves a controversial palaeoclimate problem and contributes to improving our understanding of the sensitivity of Earth's past and future climate to greenhouse gas levels and insolation. Furthermore, the large magnitude of warm pool temperature change suggests a higher tropical climate sensitivity than is found in recent-generation climate model simulations[9,11,12], which do not reproduce the magnitude of changes in sea surface temperature (Fig. 2) or the full extent of temperature changes in the troposphere. Simulations of both LGM and future climates indicate the regional climate response in the warm pool scales with the global response (Fig. 4) and therefore these palaeoclimate data may imply models that are used for simulating climate responses to changing CO_2 levels have artificially low sensitivities. A chief uncertainty in predicting future climates stems from the range of model sensitivities and therefore our results and similar Δ_{47} data sets provide an important benchmark for testing predictive models.

Methods

Modern vertical temperature profiles and snowlines. Freezing levels were estimated from four types of observation. All yield similar results and are inconsistent with an adiabat.

(1) Late-twentieth-century snowlines or equilibrium line altitudes (ELA) for Papua New Guinea (PNG) and Borneo are 4.8 km (ref. 18) and mid-twentieth-century values are 4.6–4.7 km (refs 5,6,17,28). We used late-twentieth-century mean ELA estimates of 4.60–4.80 km for glaciers in PNG and Borneo[5,6,17,18]. In the modern, the height of the ELA for tropical glaciers corresponds to the July 0 °C isotherm. In the warm pool, this isotherm does not fluctuate significantly over the course of the year. Specifically, investigation of NCEP2 data (Fig. 1), COADS data and PMIP2 model results for control and LGM simulations all show that the height of the July and annual 0 °C isotherm over PNG and Borneo does not fluctuate substantially seasonally.

(2) Extensive new quality-controlled data sets from the DOE ARM programme were used to estimate mean vertical temperature profiles for three sites varying in degree of continentality (Nauru, Manus and Darwin). Freezing levels range from 4.965 to 5.015 km (Fig. 3a).

(3) Pre-1975 radiosonde data from PNG: freezing level estimates are 4.7 ± 0.1 km (ref. 28).

(4) Terrestrial surface temperature measurements indicate values of ~4.6–4.8 km (ref. 29).

Offset between snowline and 0 °C isotherm. Owing to high rates of precipitation, tropical snowlines can be depressed to altitudes between the 0 and 1 °C isotherms[29]. NCEP2 reanalysis data show the height of these isotherms over land is similar to that over our three marine sites, with up to 0.6 °C of offset, which may also explain the small offset between estimates for the ELA and constraints on the 0 °C isotherm (Figs 1a and 3).

LGM snowlines. LGM snowlines range from 3.55 to 3.65 km above sea level (Mt Giluwe) and ~3.40–3.70 km at other sites with an average of 3.60 km. ELA (snowline) changes are calculated relative to sea level (which was ~0.12 km lower at LGM).

Clumped isotope analyses. We examined samples from three sites: MD97-2138, Ocean Drilling Program Site 806 and V24-109. Monospecific samples of

Globigerinoides ruber (white) and *Globigerinoides sacculifer* (without sac) from the >250 μm size fraction were analysed. Mean LGM SSTs were calculated from 20 clumped isotope (Δ_{47}) analyses of planktic foraminifera and coccoliths. Δ_{47} refers to the ‰ excess of $^{13}C^{18}O^{16}O$ in CO_2 (produced from sample acid digestion), compared with the amount that is predicted to be present if isotopes were randomly distributed among all possible isotopologues of CO_2. Each foraminiferal analysis represents the average of several hundred to a few thousand individuals, and each bulk sediment analysis is composed of tens of thousands or more coccoliths. Little seasonal temperature variation is observed (or expected) in the warm pool or in the production of these carbonate-secreting organisms. To study regional hydrology, we reconstructed $\delta^{18}O_w$ using paired measurements of carbonate $\delta^{18}O$. $\delta^{18}O_w$ is reported in units of ‰ relative to the Vienna Standard Mean Ocean Water standard.

Although errors in individual sample measurements for Δ_{47} temperatures are larger than what is typically reported for some other proxies (> 1 °C), by measuring replicate samples, we are able to reduce this source of uncertainty to < 1 °C. Other sources of uncertainty stem from how representative measurements of samples are of the mean for a region, and for the time interval being studied. Owing to the large sample sizes, our results should reflect a long-term regional mean for the LGM, despite the limited temporal resolution of our records. For consistency with the MARGO synthesis, we compared LGM proxy SSTs with climatological values[22]. LGM temperatures are 25.3 ± 0.4 °C (2 s.e.m.). The LGM–climatology difference is 4.1 ± 0.4 °C (2 s.e.m.) and the LGM–coretop difference is 4.7 ± 0.8 °C (2 s.e.m.).

Radiative–convective calculations of temperature profiles. To calculate tropospheric temperature profiles, we created a procedure[27] as close as feasible to the simplicity of a moist adiabat but which takes into account the impact of entrainment of environmental air in the troposphere. Although the moist adiabat requires specification only of near-surface air temperature and specific humidity, we also specify relative humidity as a function of height for these calculations. Environmental temperatures above the boundary layer are calculated as a modified radiative–convective equilibrium using a modified Betts–Miller convective scheme[30] that adjusts temperatures towards that of the entraining convective plume. To consider the effects of entrainment on vertical temperature profiles, we needed a model that computes its temperature interactively as we go up from the surface, including temperature inside and outside the plume. A convective adjustment scheme was chosen because it is one of the simplest convective models for such computations and has the advantage that the assumptions are very transparent. We conducted sensitivity tests to consider effects of changing SSTs, entrainment coefficient, surface relative humidity and FTRH values on predicted snowlines, and tested different specifications of the change in relative humidity including generating highly conservative error bars based on thresholds associated with convection.

Received 4 October 2013; accepted 7 January 2014; published online 27 February 2014

References

1. CLIMAP Project Members, The surface of the ice age earth. *Science* **191,** 1131–1137 (1976).
2. MARGO Project Members, Constraints on the magnitude and patterns of ocean cooling at the Last Glacial Maximum. *Nature Geosci.* **2,** 127–132 (2009).
3. Lea, D., Pak, D. & Spero, H. Climate impact of Late Quaternary equatorial Pacific sea surface temperature variations. *Science* **289,** 1719–1724 (2000).
4. De Garidel-Thoron, T. *et al.* A multiproxy assessment of the western equatorial Pacific hydrography during the last 30 kyr. *Paleoceanography* **22,** PA3204 (2007).
5. Porter, S. Snowline depression in the tropics during the last glaciation. *Quat. Sci. Rev.* **20,** 1067–1091 (2001).
6. Hastenrath, S. Past glaciation in the tropics. *Quat. Sci. Rev.* **28,** 790–798 (2009).
7. Farrera, I. *et al.* Tropical climates at the Last Glacial Maximum: A new synthesis of terrestrial palaeoclimate data. I. Vegetation, lake-levels and geochemistry. *Clim. Dynam.* **15,** 823–856 (1999).
8. Betts, A. & Ridgway, W. Tropical boundary layer equilibrium in the last ice age. *J. Geophys. Res.* **97,** 2529–2534 (1992).
9. Braconnot, P. *et al.* Results of PMIP2 coupled simulations of the mid-Holocene and Last Glacial Maximum—part 1: Experiments and large-scale features. *Clim. Past* **3,** 261–277 (2007).
10. Braconnot, P. *et al.* The Paleoclimate Modeling Intercomparison Project contribution to CMIP5. *CLIVAR Exchanges* **56,** 15–19 (2011).
11. Braconnot, P. *et al.* Evaluation of climate models using palaeoclimatic data. *Nature Clim. Change* **2,** 417–424 (2012).
12. Otto-Bliesner, B. *et al.* A comparison of PMIP2 model simulations and the MARGO proxy reconstruction for tropical sea surface temperatures at Last Glacial Maximum. *Clim. Dynam.* **32,** 799–815 (2009).
13. Mathien-Blard, E. & Bassinot, F. Salinity bias on the foraminifera Mg/Ca thermometry: Correction procedure and implications for past ocean hydrographic reconstructions. *Geochem. Geophys. Geosyst.* **10,** Q12011 (2009).
14. Beck, J. *et al.* Sea-surface temperature from coral skeletal strontium/calcium ratios. *Science* **257,** 644–647 (1992).
15. Stute, M. *et al.* Cooling of tropical Brazil (5 °C) during the Last Glacial Maximum. *Science* **269,** 379–383 (1995).
16. Xu, K. & Emanuel, K. Is the tropical atmosphere conditionally unstable? *Mon. Weath. Rev.* **117,** 1471–1479 (1989).
17. Barrows, T., Hope, G., Prentice, M., Fifield, L. & Tims, S. Late Pleistocene glaciation of the Mt Giluwe volcano, Papua New Guinea. *Quat. Sci. Rev.* **30,** 2676–2689 (2011).
18. Prentice, M. & Glidden, S. in *Altered Ecologies: Fire, Climate and Human Influence on Terrestrial Landscapes* Vol. 32 (eds Haberle, S. G., Stevenson, J. & Prebble, M.) 457–471 (ANU EPress, 2010).
19. Hostetler, S. & Clark, P. Tropical Climate at the Last Glacial Maximum Inferred from Glacier Mass-Balance Modeling. *Science* **290,** 1747–1750 (2000).
20. O'Gorman, P. & Muller, C. How closely do changes in surface and column water vapor follow Clausius–Clapeyron scaling in climate change simulations? *Environ. Res. Lett.* **5,** 025207 (2010).
21. Tripati, A. *et al.* ^{13}C–^{18}O isotope signatures and 'clumped isotope' thermometry in foraminifera and coccoliths. *Geochim. Cosmochem. Acta* **74,** 5697–5717 (2010).
22. Reynolds, R. *et al.* An improved in situ and satellite SST analysis for climate. *J. Clim.* **15,** 1609–1625 (2002).
23. Visser, K., Thunell, R. & Stott, L. Magnitude and timing of temperature change in the Indo-Pacific warm pool during deglaciation. *Nature* **421,** 152–155 (2003).
24. Elderfield, H. *et al.* A record of bottom water temperature and seawater $\delta^{18}O$ for the Southern Ocean over the past 440 kyr based on Mg/Ca of benthic foraminiferal *Uvigerina* spp. *Quat. Sci. Rev.* **29,** 160–169 (2010).
25. Brown, R. & Zhang, C. Variability of Midtropospheric Moisture and Its Effect on Cloud-Top Height Distribution during TOGA COARE. *J. Atmos. Sci.* **54,** 2760–2774 (1997).
26. Kuang, Z. & Bretherton, C. A Mass-Flux Scheme View of a High-Resolution Simulation of a Transition from Shallow to Deep Cumulus Convection. *J. Atmos. Sci.* **63,** 1895–1909 (2006).
27. Holloway, C. & Neelin, J. Moisture vertical structure, column water vapor, and tropical deep convection. *J. Atmos. Sci.* **66,** 1665–1683 (2009).
28. Prentice, M., Hope, G., Maryunani, K. & Peterson, J. An evaluation of snowline data across New Guinea during the last major glaciation, and area-based glacier snowlines in the Mt. Jaya region of Papua, Indonesia, during the Last Glacial Maximum. *Quat. Inter.* **138,** 93–117 (2005).
29. Prentice, M. & Hope, G. in *The Ecology of Papua* (eds Marshall, A. J. & Beehler, B. M.) 177–195 2007).
30. Betts, A. & Miller, M. A new convective adjustment scheme. Part II: Single column tests using GATE wave, BOMEX, ATEX and arctic air-mass data sets. *Q. J. R. Meteorol. Soc.* **112,** 693–709 (1986).

Acknowledgements

A.K.T. would like to thank L. Thompson, R. Alley, A. Carlson, F. Anslow, D. Cicerone, D. Lea, N. Meckler, T. Schneider, S. Bordoni, K. Emanuel, J. Adkins, T. Crowley, T. Merlis and H. Spero for discussions; S. Crowhurst, H. Elderfield, A. LeGrande, G. Schmidt and L. Yeung for discussion of this work and comments on an early draft of this manuscript; J. Booth and L. Booth for invaluable assistance with sample preparation; J. Eiler for access to his laboratory and discussion of the work; and T. de Garidel-Thoron for provision of published data from MD97-2138. A.K.T. acknowledges J-Y. Peterschmitt and J. Meyerson for assistance extracting climate model outputs and drafting figures, and the international modelling groups that participated in PMIP2 and CMIP5 for providing their model output for analysis. We thank C. Holloway for the entrainment calculation code. Support was provided to A.K.T. by NSF (CAREER award, EAR-0949191, ARC-1215551), DOE (DE-FG02-13ER16402), the Hellman Foundation, NERC, and the UCLA Division of Physical Sciences; to R.A.E. by NSF (ARC-1215551); and to J.D.N. by NSF (AGS-1102838), which supported S.S. Sounding data for the warm pool are from the DOE Atmospheric Radiation Measurement Climate Research Facility. Support for the NCEP2 (Twentieth Century Reanalysis Project) data set is provided by DOE and NOAA, and for the Reynolds Ocean Temperature Reanalysis Dataset is provided by NOAA. Sediment samples were obtained from the Ocean Drilling Program and CEREGE.

Author contributions

A.K.T. designed the project and experiments, managed the project, measured most of the samples, guided the modern data analysis, adiabat calculations, initiated the collaboration with modellers, interpreted the results and wrote the manuscript with feedback from all authors. R.A.E. assisted with project design and measured some of the samples. D.P. and S.S. analysed the modern sounding data and conducted the radiative–convective equilibrium calculations under the supervision of J.D.N., J.L.M. and A.K.T. L.B. provided samples from MD97-2138.

Additional information

Supplementary information is available in the online version of the paper. Reprints and permissions information is available online at www.nature.com/reprints. Correspondence and requests for materials should be addressed to A.K.T.

Competing financial interests

The authors declare no competing financial interests.